Alignment Process for Glass Substrates Using Electrostatic Self-Assembly

M. Stucki[1,2*], C. Schumann[1,2] and A. Raatz[1,2]

[1] Leibniz University Hannover, Institute of Assembly Technology,
An der Universität 2, 30823 Garbsen, Germany
[2] Cluster of Excellence PhoenixD (Photonics, Optics, and Engineering –
Innovation Across Disciplines), Hannover, Germany
*Corresponding stucki@match.uni-hannover.de

Abstract. Sequential precision placing and bonding of components is time-consuming and expensive. Electrostatic self-assembly is a process for the parallel alignment of flat parts. Fluid between the parts acts as bearing and dielectric and serves as an adhesive for the subsequent bonding process. After a rough pre-positioning, a voltage leads to the electrical attraction between electrodes on both components. This results in a force that precisely aligns the parts on the designated assembly position. This paper describes the basics of the electrostatic self-assembly process and presents a structure design for the alignment of large-scale parts (127 mm). A model would help to design necessary conductive structures and control the process. In order to build a suitable model, we investigate the correlation between the applied voltage, the positioning error and velocity during the alignment process. We present the temporal velocity distribution in the process and calculate the alignment force based on a simple theoretic model.

Keywords: Precision Alignment, Self-Assembly, Parallel Assembly.

1 Introduction

Optical systems are used in a lot of growing markets, like communication technology and consumer electronics such as wearables [1]. However, the manufacturing processes of electronics and optical technologies are difficult to combine and currently sequential handling processes are very common. With high precision requirements for optics, this process is very expensive [2]. Therefore, the Institute of Assembly Technology is researching strategies for the effective assembly of optical devices within the PhoenixD Cluster of Excellence. The authors are transferring previous research on electrostatic self-assembly to optical systems [3–6]. Instead of aligning micro components, the process is adapted to a larger scale. To enable this technology for batch processes, the concept includes the alignment of full wafers. Basic correlations between positioning accuracy and input parameters like the applied voltage are already known by the research on microelectromechanical systems (MEMS). To expand the understanding of the process, we developed a concept for aligning large components and carried out a series of experiments. We investigate if the modelling for MEMS is also valid for larger

scales and suitable for optical components. Several criteria can be taken into account, but the focus is on the alignment force. This was determined for MEMS in the µN-scale [7] and can hardly be measured directly. Therefore, we use the velocity during the process to approximate the alignment force using a fluid dynamic model.

2 Self-Assembly by Electrostatic Forces

So far, in particular BÖHRINGER, DALIN and WILDE et al. researched in the field of self-assembly for micro components and MEMS. BÖHRINGER was very active in the field of capillary self-assembly from 1995 to 2005 and established important concepts for electrostatic self-assembly [8]. The researchers DALIN and WILDE researched the assembly of MEMS until 2015 [3–5]. They described the principle of electrostatic self-assembly with wired pads as adapted by the authors in this paper.

In this paper, we address electrostatic self-assembly as a technique for the precise alignment of two flat components (top and bottom part). For this purpose, electrically conductive structures are deposited on both components. These structures consist of conductive tracks and surfaces called pads. The top part floats on a liquid that also serves as an insulator and dielectric [7]. Two facing pads form a plate capacitor. A voltage at the lower component charges the pads with different polarity. Due to the Coulomb force, a charge shift also occurs in the upper part with inverted polarity. The oppositely charged pads attract each other through the electrostatic force. This force acts in the transverse and lateral directions. The alignment force F_{al} is the result of the lateral forces, which leads to a movement in the planes. DALIN and WILDE discovered that the alignment works better with AC than with DC and presumed, this occurs due to sticking effects of the parts [3]. Fig. 1 shows this concept based on a simple design.

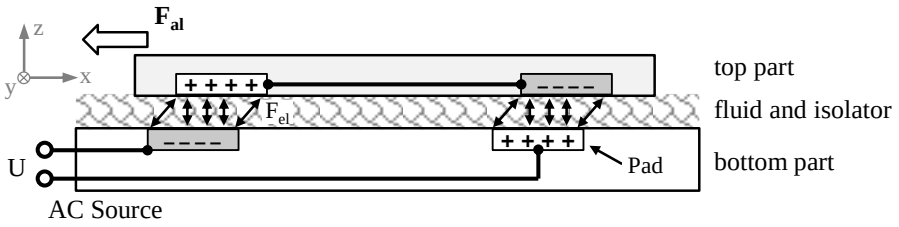

Fig. 1. Concept of electrostatic self-assembly

Building a self-assembly system requires a systematic structural design for the pads and conductive tracks. In their research, DALIN and WILDE focused on small components with an edge length of up to 10 mm. The deposited pads had an edge length of a few 100 µm. The structures were evenly arranged over the entire surface of the component [4–7]. The structural design process includes three steps, the determination of the pad-geometry (geometric shape of the single pads), the pad-arrangement (the positioning of the pads in relation to each other) and interconnection. The example in Fig. 2 shows an altering connection.

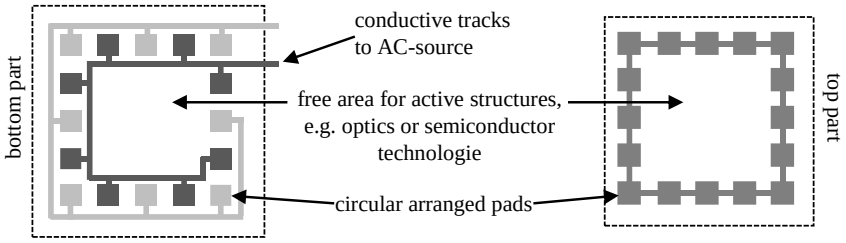

Fig. 2. Example of a square structure design with altering wired pads

DALIN and WILDE build up simulations on a single pair of square pads with a one-dimensional offset to identify the most important correlations between the system parameters and the alignment force F_{al} [9]. The alignment force:

- increases proportionally with the edge length of the pad W
- increases with the square of the applied voltage V
- is inversely proportional to the distance between the two components h
- depends on the offset O, i.e. the middle distance of the pads

The simulation results lead to the following model adapted from [9]:

$$F_{al} = -\frac{W\varepsilon_o\varepsilon_r V^2}{4h} \cdot e^{-\left(-0.8+\frac{W}{O}\right)^2} \tag{1}$$

3 Concept and Structure Design

For the assembly of optical devices, the task of electrostatic alignment changes in some aspects. Assembling many components with a self-assembly process still requires a sequential pre-positioning on the bottom part (e.g. substrate). To bypass this time-consuming placing process, we pursue the approach of aligning significantly larger components that serve as carriers for optical and electrical components. Because electrical components like photo sensors are usually processed on wafers, we use this as a reference size. With this concept, we chose a different approach than other researches so far and align several components at the same time without sequential handling.

Optical components are not conductive, therefore they must be deposited next to the self-assembly structures. This requires significant changes to the previous structural designs, which were developed for micro components. The example structure design in Fig. 2 already shows a suitable arrangement with free area for active structures. Because of the significantly larger components, the geometry of the pads has to be scaled up to create the required alignment forces. The alignment structure consists of rectangular pads with a surface of 1 x 5 mm² each. We arranged 76 pads in a circle with a diameter of 105 mm, to generate as much free space as possible in the center of the wafer. The interconnection of the bottom wafer leads to an alternating charge. We placed reference structures for the measurement of the positioning error in the center. Fig. 3 shows the full structure design used in this paper. The smaller circular arrangement of pads exist for another test series and was not used in the following experiments.

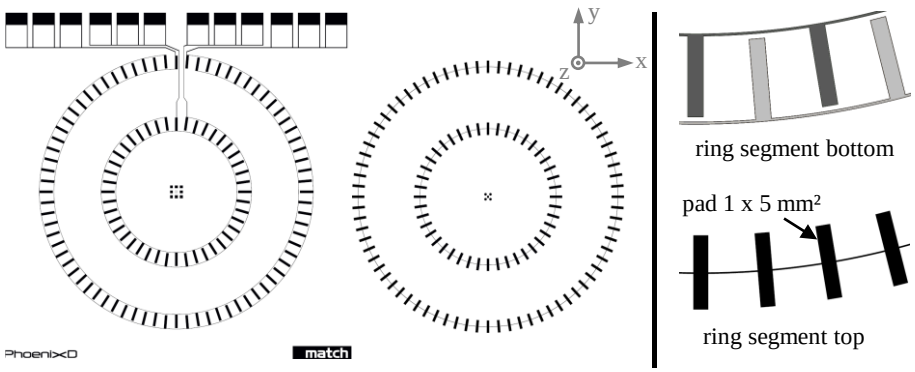

Fig. 3. Structure design for wafer alignment

4 Experimental Setup

In the experiments, we apply a voltage to the test structures and measure the positioning error based on the deviation of the measurement structures with a camera. We describe the process in more detail at the end of the experimental setup. For the alignment, we use rectangular lithography masks as test components. These masks consist of soda-lime glass and are pre-coated with a chromium layer of 100 nm. This coating is structured with the structure design (Fig. 3). The bottom mask has a side length of 15.25 cm (~6 inches) while the top mask has 12.7 cm (~5 inches) and a thickness of 560 µm. Placing them on top of each other leaves an uncovered surface area for the galvanic connection with contact tips on the bottom mask.

In the experimental setup, the bottom mask lies on a planar backlight. Central above the measurement structures we mounted a 6.4 MP camera (IDS 3880 CP) with a 4x telecentric zoom lens and additional coaxial illumination. The optical resolution of the measurement system is 0.6 µm/px, confirmed by a separate measurement. We evaluated the camera images with the Open Source Computer Vision Library (OpenCV). We use grayscale analyses and the Canny edge algorithm to detect the measurement structures. The measuring system's overall resolution is enhanced by using sub-pixel interpolation and mean values. A monitor allows the in situ observation of the alignment process. To reduce mechanical vibrations that would affect the measurement, the whole setup is placed on a damping plate. An additional confocal distance sensor (microEpsilon IFS2405-3) allows the measurement of the surface, which allows the calculation of the gap height h between these wafers (thickness of the fluidic layer). The current setup is not suitable for performing this measurement in situ; instead, we measure the gap height directly after the pre-positioning of the top part. A function generator (GW-Insteck ASR 2050) supplies the voltage up to 350 V directly to the contact tips. With an interposed transformer, a voltage up to 3500 V is possible. Fig. 4 shows an overview and detail of the experimental setup.

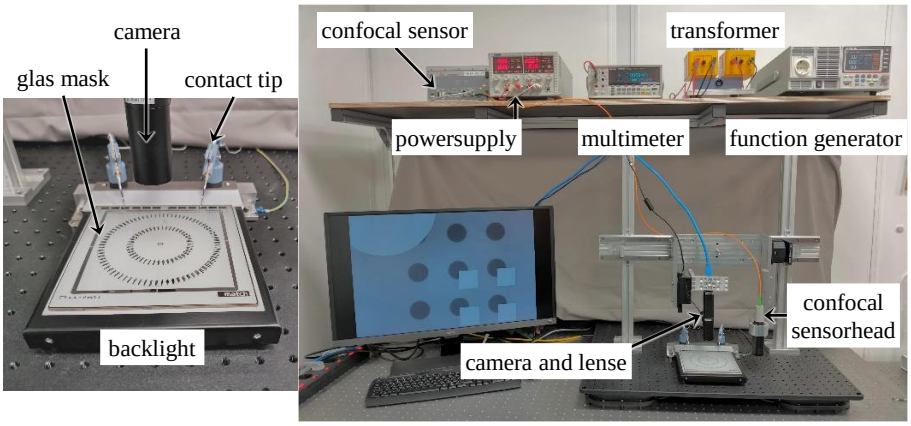

Fig. 4. : Experimental setup: detail (left) – overview (right)

At the beginning of a test series, we measure the surface of the bottom part with the confocal sensor. Then we apply the fluid and place the top part. We measure the surface again to calculate the thickness of the fluid layer. This varies between 70 µm and 100 µm. The fluid is the acrylic-based UV adhesive Sicuwell 7043-N with a viscosity η ~80 mPA/s (23° C). High transparency allows measurement through the glass and fluid layer. Curing the adhesive by UV light is anticipated in the process, but not part of our experiments. The manual placing process of the top part results in an initial positioning error between 450 µm and 700 µm in x- and y-direction. The electrostatic alignment starts without any measurable delay after activating the voltage. The component aligns on the assembly position and the voltage is deactivated. For each set of parameters, we repeat this process 10 times. During the alignment, the camera takes a video of the measurement structures for later evaluation.

4.1 Evaluation criteria

Common evaluation criteria are the success rate of the positioning and the positioning error. While the success rate quantifies only if an alignment happened, the positioning error describes the accuracy of the process. We measure the positioning error in *x*-direction e_x and *y*-direction e_y and calculate the absolute positioning error *d* as the vector length of e_x and e_y. The alignment force F_{el} is a relevant factor. TONDORF et.al. calculated the alinement force in the µN-scale [7]. Therefore, this variable is hard to measure directly and we take a theoretic approach to calculate the value. The model from DALIN's simulation is one option, but cannot be directly transferred to larger components and a multi-dimensional task. Instead, we calculate the alignment force with a common fluid dynamic model (2). The gap height *h* and velocity v are measured within the experimental setup. The surface area *A* and the viscosity η are known from the components and product information of the adhesive.

$$F = \eta \frac{v\,A}{h} \tag{2}$$

5 Results and Discussion

In the test series, we investigated the influence of the input voltage on the positioning error and velocity. We measured the single frames of the videos taken by the camera and plotted the results in a diagram. Fig. 5 shows a typical plot with the errors e_x, e_y and d. The velocity v in µm/s is a smoothed curve (median over 10 values).

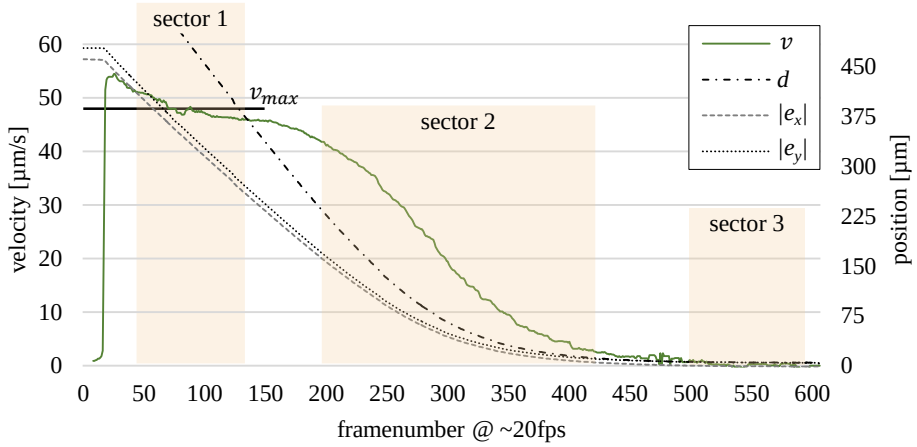

Fig. 5. Plot of the positioning errors e_x, e_y, d and the velocity v

We separate the movement into three sectors. The width of the sectors varies depending on the total duration of the process. In sector 1, the movement is almost linear and we calculate the highest velocity v_{max} as a mean value, leaving out the initial peak. In sector 2 the velocity reduces while the part approaches the assembly position. The positioning errors ascend asymptotically to the final value in sector 3.

The asymptotic approximation fits the simulation model of DALIN et al. The inverted overlap of the pads $\frac{W}{o}$ is an exponential factor in equation (1), meaning lateral alignment force decreases with the overlap. When the process starts, the overlap is small and increases when the positioning error gets smaller during the process. With the increasing overlap, the lateral force decreases during the alignment. At the assembly position ($d = 0$µm) the overlap is 100% and the alignment force F_{al} = 0 N.

The experiments cover the voltage level in the range of 250 V and 1250 V (sine wave, 50 Hz). Even with the high initial error of up to 700 µm by the pre-positioning, the success rate over all experiments is 100%. Fig. 6 left shows the correlation between the voltage level and the absolute positioning error. The error decreases significantly between 250 V and 750 V. The minimum is 0.4 µm with a standard deviation of 0.2 µm, but the measuring system reaches its limit at this scale. With higher voltage, the positioning error increases. Most likely, this effect occurs due to higher attraction between the components (z-direction), which reduce the thickness of the adhesive layer and leads to higher friction. However, an in situ measurement of the thickness is not possible with the given setup.

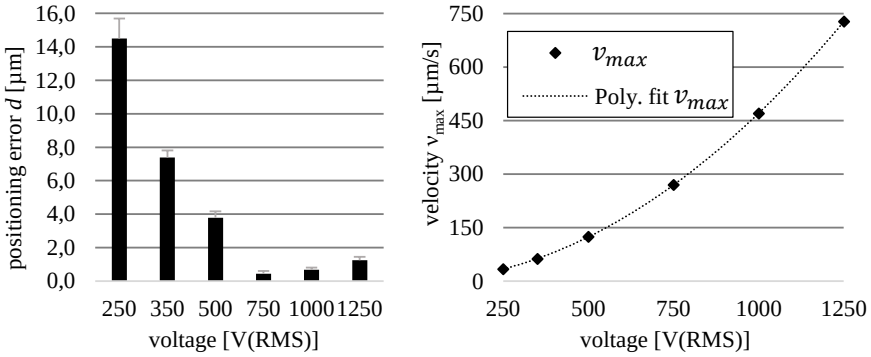

Fig. 6. Correlation between the AC-voltage and the absolute positioning error (left) and the maximum velocity (right). Data from Table 1.

The maximum velocity v_{max} continuously increases from 34 µm/s at 250 V up to 727.3 µm/s at 1250 V (Fig. 6-right). According to equation (2), the correlation between the velocity and the alignment force F_x is linear. Therefore, the curve for the alignment force is equal to the velocity and the qualitative result is identical. A polygon of the second degree approximates the measurements very closely. This fits with the simulation model of DALIN et al. (1) that also has the voltage as a squared factor for the alignment force. Table 1 contains the data of our experiments and the calculated forces (with a mean gap height h = 89 µm, viscosity $\eta = 80\,\frac{mPa}{s}$ and surface area A = 161.29 cm²).

Table 1. Positioning errors, maximum velocity and calculated alignment force

voltage	error e_x	error e_y	error d	v_{max}	$\lvert F_x \rvert$
250 V	-10.3 µm	-10.2 µm	14.5 µm	34.0 µm/s	0.5 mN
350 V	-6.4 µm	-3.7 µm	7.4 µm	62.5 µm/s	0.9 mN
500 V	-3.1 µm	-2.2 µm	3.8 µm	124.6 µm/s	1.8 mN
750 V	-0.3 µm	-0.3 µm	0.4 µm	269.7 µm/s	3.9 mN
1000 V	0.6 µm	0.3 µm	0.7 µm	469.7 µm/s	6.8 mN
1250 V	0.9 µm	0.9 µm	1.2 µm	727.3 µm/s	10.5 mN

The position error has a minimum at 750 V, but the speed increases continuously. The already mentioned effect of an increasing attraction in the z-direction with the higher voltage occurs primarily with a large overlap of the structures. At the time we measure v_{max}, the overlap is minor compared to the end of the process when the position error is determined. Therefore, this effect influences the positioning error more than v_{max}. Nevertheless, for modelling this effect, the gap height has to be measured in situ to validate the theoretic approach.

6 Conclusion and outlook

In this paper, we present a technique of electrostatic self-assembly for the precise alignment of optical devices. Until now, the research had the focus on small electrical devices like MEMS. Our approach addresses the alignment of larger parts with multiple

electric and optical elements to create a batch process for wafer-based technology devices. For this, we created a structure design suitable for 5” wafers.

The focus of this paper is the correlation of the applied voltage, the positioning error and velocity during the alignment process. While the positioning error is the most recent evaluation criterion, the velocity allows the calculation of the alignment fore that is needed for a simulation in future work. Within the test series, we aligned a 125 mm square glass part using voltages between 250 V and 1250 V. The success rate over the series was 100%. The minimum absolute positioning error d was 0.4 µm with 750 V, a 105 mm alignment structure and 50 Hz altering current. The velocity has a maximum (v_{max}) at the beginning of the alignment process. v_{max} increases continuously by the square of the applied voltage and reaches up to 727.3 µm/s at 1250 V. We calculated the alignment force F_x up to 10.5 mN, under the preconditions that gap height is constant and the velocity distribution is even. Further research focuses the detailed modelling of the alignment force. Therefore, the experimental setup will be enhanced to provide a higher frame rate and in situ measurement of the gap height. This enables a better temporal resolution and accurate calculation of the alignment force for the simulation. With this simulation, we plan to build a computer-aided structural design and develop special structures with orientated force distribution that adapt to the assembly task.

References and Acknowledgements

The research in this paper is funded by the Deutsche Forschungsgemeinschaft (DFG, German Research Foundation) under Germany’s Excellence Strategy within the Cluster of Excellence PhoenixD (EXC 2122, Project ID 390833453). The authors thank the German Research Foundation (DFG) for their support.

1. Vinciguerra, S., Vinciguerra, M.: Smart devices and healthy aging. NHA (2019).
2. Srinivasan, U., Helmbrecht, M.A., Muller, R.S., Howe, R.T.: MEMS: Some Self-Assembly Required. Optics & photonics news 13, 20–25 (2002)
3. Dalin, J., Wilde, J.: Self-assembly of micro-parts using electrostatic forces and surface tension. In: 59th Electronic Components and Technology Conference, (2009).
4. Dalin, J., Wilde, J., Lazarou, P., Aspragathos, N.: Self-assembly of dies through electrostatic attraction: modelling of alignment forces and kinematics. J. Micro-Nano Mech. (2011).
5. Dalin, J., Wilde, J., Zulfiqar, A., Lazarou, P., Synodinos, A., Aspragathos, N.: Electrostatic attraction and surface-tension-driven forces for accurate self-assembly of microparts. Microelectronic Engineering (2010).
6. Tondorf, M., Gan, Y., Mouselimis, K., Wilde, J.: Elektrostatisch-fluidische Selbstassemblierung für die hochgenaue Mikro-Montage von MEMS. Elektronische Baugruppen und Leiterplatten DVS Berichte, 46–51 (2014)
7. Tondorf, M., Wilde, J.: Elektrostatische und fluidische Self-Assembly-Prozesse für die präzise Montage von Mikrosystemen. Schlussbereicht zu dem IGF-Vorhaben (2015)
8. Bohringer, K.-F., Goldberg, K., Cohn, M., Howe, R., Pisano, A.: Parallel microassembly with electrostatic force fields. IEEE International Conference on Robotics and Automation, Leuven, Belgium, 16-20 May 1998, pp. 1204–1211.
9. Dalin, J., Wilde, J., Synodinos, A., Lazarou, P., Aspragathos, N.: Concept for Fluidic Self-Assembly of Micro-Parts Using Electro-Static Forces (2008)